HiSST: 3rd International Conference on
High-Speed Vehicle Science Technology
14 -19 April 2024, Busan, Korea

Design and Commissioning of TNO's modular Rotating Detonation Engine (RDE) test facility

Tim Roos[1], Wolter Wieling[2], Moana Lengkeek[3], Martin Olde[4]

Abstract

Rotating detonation engines are an effective means of utilising detonation combustion in a wide variety of (aerospace) engines. The greater thermodynamic efficiency of detonative combustion, as compared to deflagrative combustion, can be used to fly farther, faster or longer with the same amount of fuel, an attractive prospect in many applications. This work reports on the design of an RDE test facility at TNO in the Netherlands, that was set up to facility research efforts on this promising technology. The results of a commissioning test campaign, which includes what is believed to be the first hot fire of an RDE in the Netherlands, are also presented. The test campaign was conducted using the modular TNO RDC, which is based on a design available in the literature, operating on hydrogen and air. The pressure gain and detonation wave speed measurements obtained in the test campaign are found to compare well to the results available in the literature. Some issues were encountered with the engine diagnostics however, and alternatives to these diagnostics methods will be explored in the future. The air flow rate achieved by the facility is within 5% of the desired value, however the fuel mass flow deviated by as much as 20% from the desired value. This is likely a result of the way the fuel feed line is set up. As experience builds up this variability is expected to decrease, but it will require mitigating measures in the near future. More testing at higher mass flow rates and additional variations in engine geometry is foreseen in the future.

Keywords: *RDE, detonation, propulsion, test facility*

Nomenclature

Latin
A – Area
J – Normalised mass flow

Greek
Δ – Detonation channel gap height

Subscripts
f – fuel injector throat
3.1 – Air injector throat
4 – Detonation channel exit
8 – Nozzle throat

1. Introduction

Rotating detonation engines (RDE) have been the subject of significant research efforts all over the world, in particular over the last decade. They provide a means of leveraging the significantly greater thermodynamic efficiency of detonative combustion over deflagrative combustion in a variety of propulsion systems, ranging from rocket engines to turbine engines. The greater power density of RDEs, as well as their quasi-steady outflow, make RDEs an attractive option when compared to

[1] *TNO Defense, Safety & Security, Ypenburgse Boslaan 2, 2496 ZA The Hague, tim.roos@tno.nl*
[2] *TNO Defense, Safety & Security, Ypenburgse Boslaan 2, 2496 ZA The Hague, wolter.wieling@tno.nl*
[3] *Technische Universiteit Delft, Kluyverweg 1, 2629 HS Delft, m.n.lengkeek@student.tudelft.nl*
[4] *TNO Defense, Safety & Security, Ypenburgse Boslaan 2, 2496 ZA The Hague, martin.olde@tno.nl*

Copyright © 2024 by author(s)

deflagration engines or other types of detonation engines (e.g. pulse detonation engines), respectively.

Given the potentially significant efficiency enhancements offered by RDEs an exploratory research effort into the technology has been initiated at TNO in The Netherlands. This effort has thus far primarily focused on gaining hands-on experience with detonation combustion, through the development of test infrastructure and a work-horse combustor test bed. This paper will report on the activities that have been conducted so far, including what is believed to be the first hot fire of a rotating detonation combustor in The Netherlands.

The combustor test bed and test facility will first be described, together with the instrumentation set-up that has been used thus far. The results of a short test campaign, conducted with the purpose of commissioning the facility and achieving a successful hot fire, will then be presented and analysed. Using these results several possible improvements to the facility will be identified, and plans for future work will finally be discussed.

2. Experimental set-up

2.1. TNO RDC

The TNO Rotating Detonation Combustor (RDC), hereafter referred to as the TNO RDC, is based on the modular RDC developed at the TU Berlin [1, 2, 3], which in turn was based on the design by Shank [4]. It is termed a combustor instead of an engine because it does feature a proper nozzle, although the test facility described in this work can also be used to test RDEs.The TNO RDC was made stronger than the previous design, to allow for testing at higher mass flows and pressures. Specifically, the propellant plena were designed to handle pressures of up to 100 bar.

The RDC features jet-in-crossflow fuel injection where the oxidiser is injected radially inward through a slot with a height d_{air} and fuel is injected axially through a number of discrete holes with diameter d_j. A cross section of the engine is presented in Figure 1. The station definition presented in [5] for airbreathing RDEs is used to denote the engine stations, with station 2 denoting the air plenum, station 3.1 denoting the air injector throat, station 3.2 detonating the base of the detonation channel, station 4 denoting the end of the detonation channel and station 8 denoting the nozzle throat.

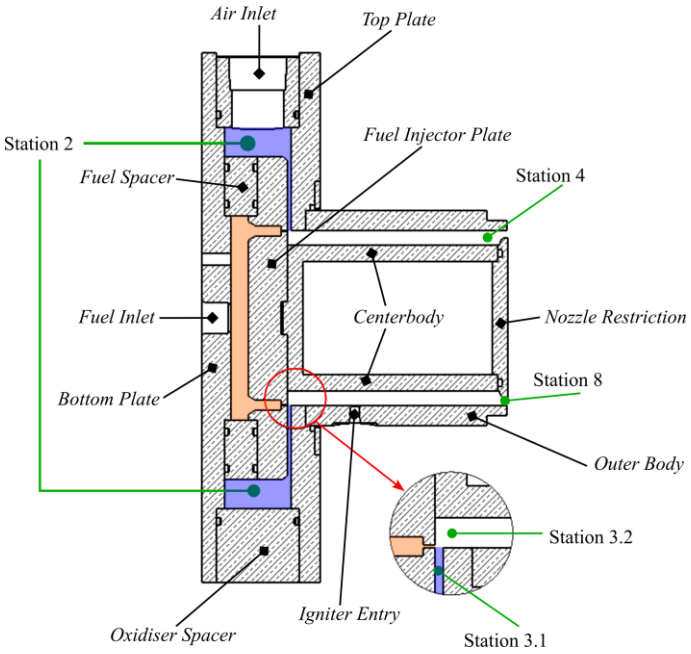

Figure 1 Cross section of the TNO RDC. Air flowpath is show in blue, fuel flowpath is shown in orange. The various engine parts as well as the engine station definition are indicated

Copyright © 2024 by author(s)

Air is supplied to the air plenum through five 1 inch diameter holes that are evenly spaced around the RDC circumference ('Air Inlet' in Figure 1. Fuel is supplied through a single 0.5 inch diameter hole in the base of the engine ('Fuel Inlet' in Figure 1). The outer diameter of the combustor annulus is fixed at 90 mm, and the length of the detonation channel is 107.5 mm.

The engine design allows several key engine geometry parameters to be easily changed, including the air injector area ($A_{3.1}$), fuel injector area (A_f), combustor outlet restriction (1 - A_8/A_4) and detonation channel height (Δ). This allows the effect of engine geometry on engine performance and behaviour to be explored using a single device, which makes it a robust and versatile engine design that is suitable for different types of experiments.

Table 1 presents an overview of the variations in engine geometry that are possible in the TNO RDC.

Table 1 TNO RDC geometry variations

Parameter	Variations
Air injector slot height	1mm, 1.6 mm, 2 mm
Fuel injector [number of holes] x [hole diameter]	100 x 0.5 mm, 100 x 0.7 mm
Outlet restriction	0%, 25%, 50%
Channel height	7.6 mm

The detonation channel has 3 rows of diagnostics holes, spaced 120 degrees apart in the circumferential direction. Each row has 4 axially spaced access holes, spaced 25 mm apart, with the centroid of the first hole 21 mm above the top of the air injector gap. The propellant plena can also accommodate pressure and temperature diagnostics.

The engine is ignited using a hydrogen-oxygen pre-detonator operating at stoichiometric conditions that is ignited using a spark plug. The pre-detonator consists of a mixing chamber and a 200 mm long, ¼ inch diameter tube that is mounted to the engine outer body at an axial distance of 32.5 mm from the top of the air injector gap. During testing of the pre-detonator deflagration-to-detonation transition (DDT) was observed to occur inside the tube and it took 52 ms on average for the detonation wave to be deposited into the engine from the time the spark plug was triggered.

2.2. Test facility

The TNO RDC is tested at the aeropropulsion test facility at TNO Ypenburg. The test facility gas supply system (GSS) can supply up to 8.5 kg/s of air and up to 160 g/s of gaseous hydrogen at pressures of up to 80 bar. Air is supplied from a compressed air tank, whereas the hydrogen is supplied from bottle packs. The hydrogen supply line is also rated for methane.

Optionally, the air can be vitiated using a hydrogen-oxygen vitiator, downstream of which make-up oxygen is injected to maintain the correct mass fraction of oxygen. The vitiator can heat the air up to a total temperature 1000 K continuously, with a momentary peak total temperature of 1500 K. Including the make-up oxygen, the maximum vitiated air mass flow rate is 10 kg/s.

In addition to the gas supply system, the aeropropulsion test facility comprises a control system, a data acquisition system and a test bench. The control system is based on a National Instruments cDAQ-9137 with National Instruments NI 9220 analog input modules that can record 16 channels at up to 100 kHz. The acquisition system comprises 100 channels that can each be recorded at up to 100 kHz. The control system is used to administer the test and control the test facility, while the acquisition system is used to acquire part of the RDC diagnostics, as will be discussed in more detail in Section 2.3. The test-bench is located inside a test bunker, allowing for a wide variety of flow conditions and propellant types to be tested relatively easily.

Air is supplied to the TNO RDC using a 48.3 mm inner diameter tube that connects to the GSS on one end and terminates into a manifold on the other end. The hexagonal manifold features five 1 inch diameter holes, which allows the incoming air to be split into five flexible hoses. The flexible hoses are in turn connected to the air supply holes on the TNO RDC. The air mass flow is regulated by

 Copyright © 2024 by author(s)

controlling the supply pressure upstream of a metering orifice. Stagnation pressure and temperature measurements are taken upstream of this metering orifice to allow the achieved air mass flow to be calculated after each test. The air supply line is shown in Figure 2, with the key components highlighted.

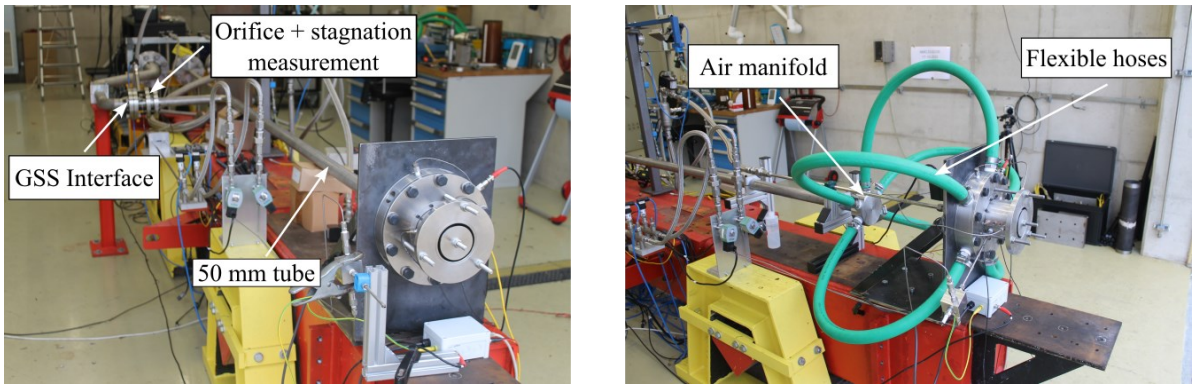

Figure 2 Air feed line for the TNO RDC feed system. The main components have been highlighted.

Fuel is supplied to the engine using a single 0.5 inch diameter line, comprising a flexible and a rigid section, with two fast-acting shut-off valves. The first valve is connected directly to the engine plenum, while the second valve is located in the GSS, several meters away from the engine. These valves, with a response time on the order of 100-200 ms, are used to control the flow of fuel to the engine and to mark the end of a test. To ensure rapid and responsive shutdown of the engine the primary shut-off valve is located as close to the engine as possible, with the second valve acting as a back-up.

Similar to the air line, the flow through the hydrogen line is metered using a metering orifice and the stagnation pressure and temperature are measured ahead of this orifice to allow the achieved fuel mass flow to be calculated after each test. The fuel flow is set by setting the fuel supply pressure. Given the length of the fuel supply line and the relatively short test times there is a lag in achieving the set pressure in the supply line, which can cause a non-negligible variability in the fuel mass flow that is achieved. This will be discussed in more detail in Section 3. The achieved fuel mass flow therefore requires close monitoring during testing. The fuel supply line is shown in Figure 3, with the key components highlighted.

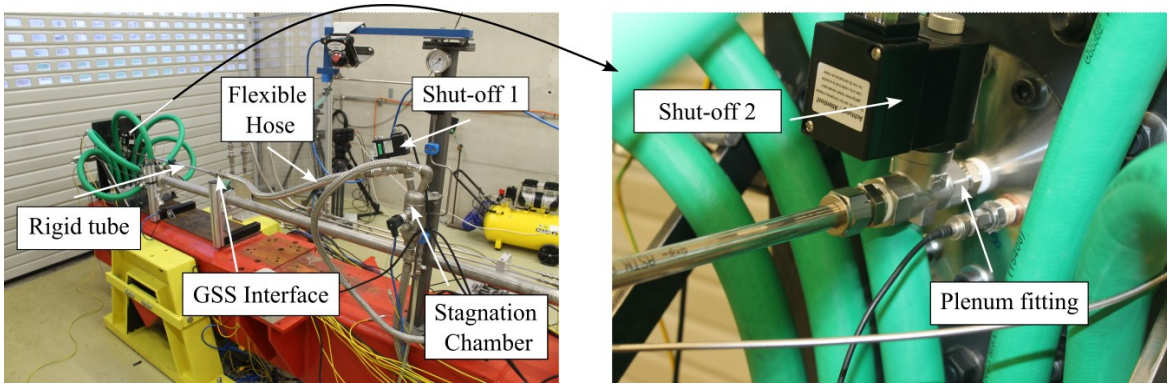

Figure 3 Hydrogen feed line for the TNO RDC feed system. The main components have been highlighted.

The pre-detonator is supplied with gaseous oxygen and hydrogen through 1/8 inch diameter lines, each of which are metered using a metering orifice. To prevent backflow of the pre-detonator combustion products into the supply lines a check valve is also included in each supply lines. The flow of propellant to the pre-detonator is controlled using two fast-acting (response time of 5-25ms)

Copyright © 2024 by author(s)

valves. As for the other supply lines, the stagnation pressure and temperature of the pre-detonator feed lines is measured to facilitate calculation of the propellant mass flows after each test. The pre-detonator is ignited using an automotive spark plug that is triggered by the facility control system.

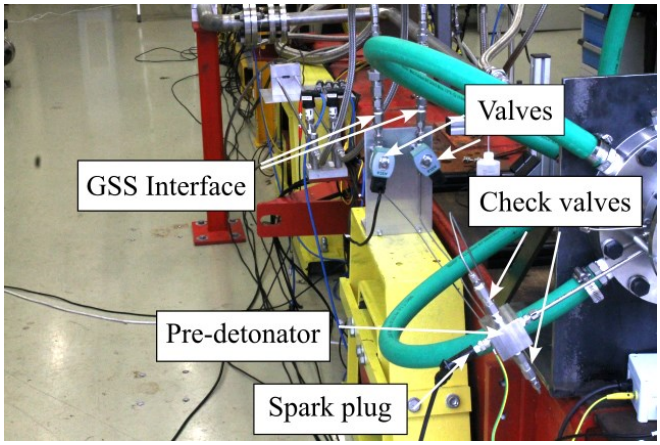

Figure 4 Pre-detonator feed system. The main components have been highlighted.

A schematic overview of the components in the RDC supply lines is provided in **Figure 5**.

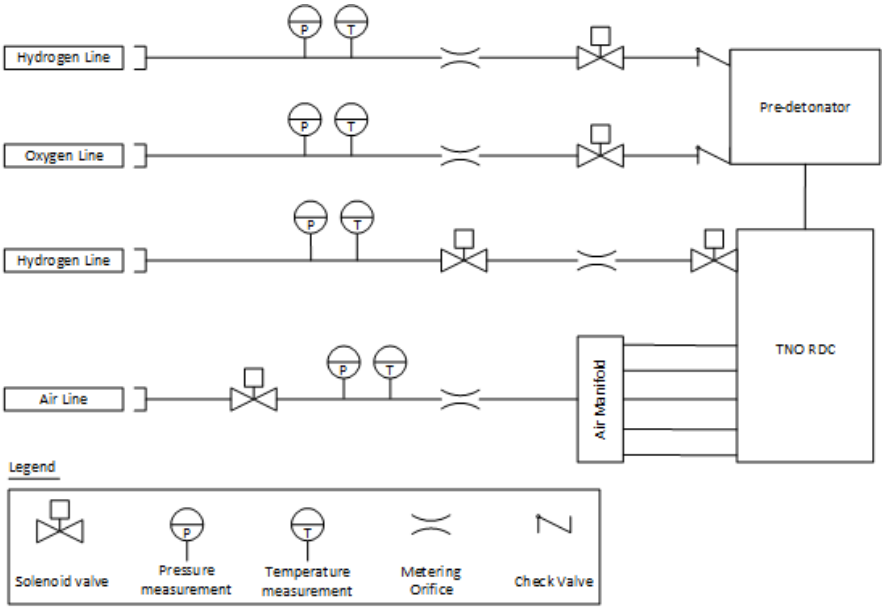

Figure 5 Schematic representation of the RDC feed system, including instrumentation

2.3. Diagnostics

The facility and RDC feature both low frequency and high frequency diagnostics. The low frequency diagnostics comprise stagnation pressure and temperature measurements in the feed system as well as the RDC propellant plena, and two Capillary Tube Attenuated Pressure (CTAP) [6] measurements mounted at the end of the detonation channel. The high frequency diagnostics currently consists of ionisation pins mounted at the base of the channel, with high frequency pressure measurements foreseen in the future.

The low frequency diagnostics are acquired at 50 kHz using the test facility DAQ. The low frequency diagnostics are recorded at 50 kHz to detect any acoustic coupling that occurs between the propellant plena and the detonation channel. Given that the maximum acquisition frequency of the DAQ system is 100 kHz, it is not suitable for acquisition of the high-frequency diagnostics. These are acquired at 500 kHz on a LeCroy Waverunner 620 Zi oscilloscope instead.

 Copyright © 2024 by author(s)

The stagnation pressure in the facility feed lines is measured using Keller PA-23SY piezo-resistive pressure sensors. Stagnation pressure in the RDC propellant plena is measured using piezo-electric Kistler 701A sensors, in order to record any acoustic coupling between the combustor plena and the detonation channel. Stagnation temperature in both the feed lines and the propellant plena is measured using K-type thermocouples.

The end of the RDC detonation channel is instrumented with two Capillary Tube Attenuated Pressure (CTAP) measurements, each consisting of a 1 m long, 1/8 inch tube that terminates in a pressure sensor. One CTAP is fitted with a piezo-electric (Kistler 701A) pressure sensor, whereas the other CTAP is fitted with a piezo-resistive (Keller PA-23SY) pressure sensor. The CTAP is used to measure the mean static pressure at the end of the detonation channel [5] and can be used to determine the pressure gain of the engine. In the present work the recorded CTAP values are corrected for Mach number using the procedure outlined in [5].

To measure the detonation wave speed the engine is instrumented with one to three (depending on the test) Dynasen CA-1041-C ionisation pins. These pins use the presence of electrons in the detonation products to detect detonation wave passage [7]. The pins are connected to a custom signal conditioning box that applies the required voltage to the pins and converts the pin output signal to a 0-5V signal that is recorded using the oscilloscope.

For some of the tests described in this work an IDTVision Y4S3 high speed camera was also used to look at the detonation wave through the RDC nozzle. The camera was found to be insufficiently sensitive to detect the relatively limited light emitted in the visible spectrum by the detonation wave however, rendering it invisible on the high-speed recording. It is therefore not considered to be part of the engine diagnostics for the remainder of this work. A conventional video camera was used to record each test however, and the sound from these test videos is used to assist in determining detonation wave speed [7].

An overview of the full RDC instrumentation and their locations is provided in Figure 6

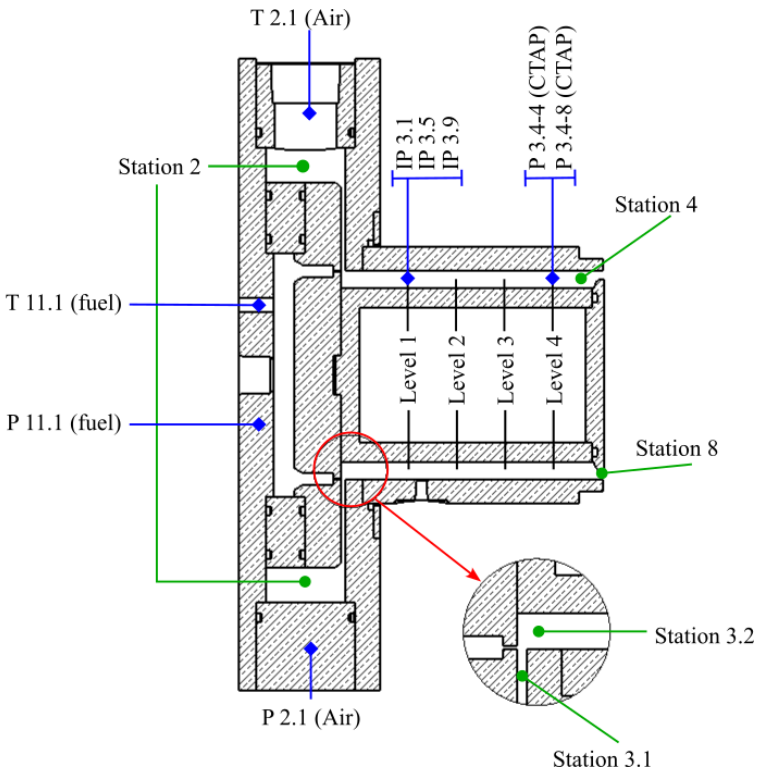

Figure 6 Overview of instrumentation and instrumentation locations on the TNO RDC.

Copyright © 2024 by author(s)

2.4. Test description

This work describes the results of a small test campaign that was conducted to commission the test facility. In this test campaign the TNO RDC was operated with air as the oxidiser and hydrogen as the fuel. A single engine configuration was used, with an air injector slot height of 1 mm, a 25% nozzle restriction and a fuel injector plate with 100 x 0.5 mm fuel injection holes. Total engine mass flow varied from 0.1 kg/s to 0.52 kg/s (51 kg/s/m^2 to 263 kg/s/m^2), with equivalence ratios varying from 0.42 to 1.2.

Fifteen tests were conducted in total. Each test had a run time of 500 ms, measured from the rising edge of the spark plug trigger signal. Of the test total test duration 150 ms is allocated for engine start, with the remaining 350 ms used as the steady-state test time.

To start the test the air supply line is opened and air is allowed to flow for 10 seconds. This allows the desired mass flow of air to be established. The RDC hydrogen feed line is then opened and hydrogen is allowed to flow for 1 second. This cold flow period enables the pressure in the hydrogen supply line to stabilise and provides a baseline CTAP reading for the unlit engine. Halfway through the cold flow period, i.e. 0.5 seconds after starting the flow of hydrogen, the pre-detonator O2 supply is also opened to fill the pre-detonator with oxidiser. At the end of the cold flow period the pre-detonator H2 supply is opened for 0.1 seconds and the spark plug is simultaneously triggered for 0.2 seconds, marking the start of the test. At the conclusion of the test the flow of hydrogen is shut off while the air continues to flow for another 10 seconds, to cool down the engine.

3. Results

Figure 7 shows the operating map for the test campaign, indicating the combinations of total mass flow and equivalence ratio that were used in the test campaign and whether the engine exhibited detonation combustion. The total engine mass flow is normalised by annulus area.

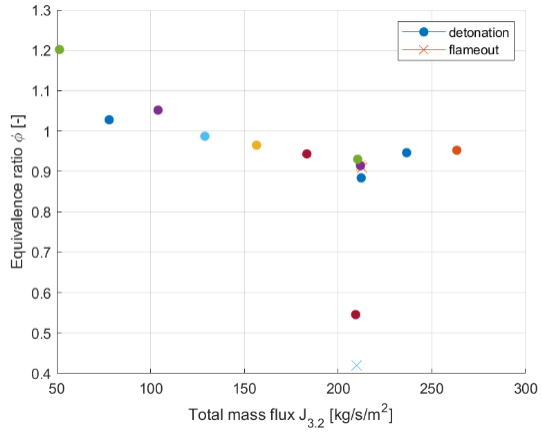

Figure 7 Operating map for the present test campaign, indicating combinations of total mass flow and equivalence ratio that were tested.

As shown in the figure the engine showed detonation combustion for 12 of the 15 tests. For two of the tests the pre-detonator failed to ignite because of an electrical issue, while for the third test the equivalence ratio (0.42) was below the detonation limit for hydrogen and air.

The target equivalence ratio was 1 for 13 of the 15 tests. For the other two tests the desired equivalence ratios were 0.4 and 0.5. From the figure, the achieved equivalence ratio was between 1.2 and 0.87 in the tests where the target equivalence ratio was 1. The variability in the achieved equivalence ratio is primarily the result of variability in the fuel mass flow the is achieved, is can be seen in Figure 8. The figure compares the desired and achieved operating point properties for each test. The black line indicates a perfect match.

 Copyright © 2024 by author(s)

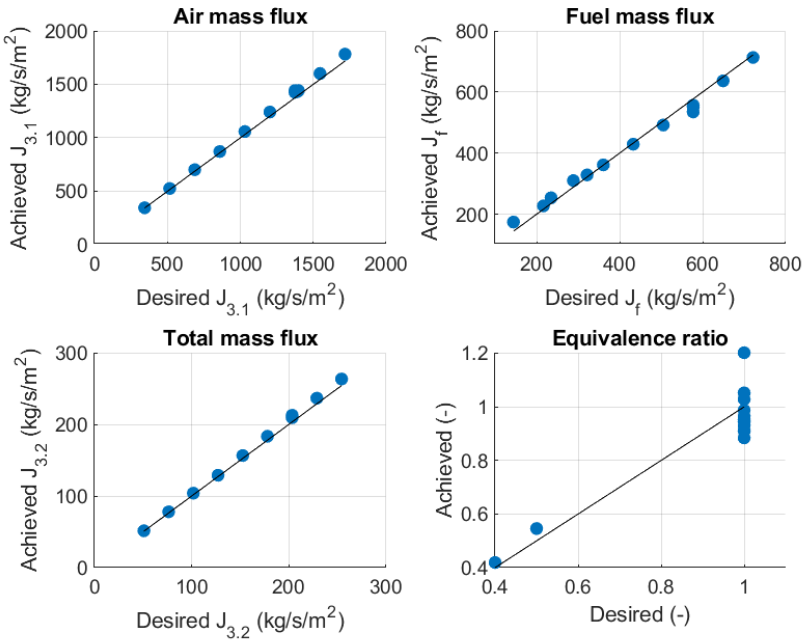

Figure 8 Comparison of achieved and desired air mass flow (top left), fuel mass flow (top right), total mass flow (bottom left) and equivalence ratio (bottom right) for all tests.

From the figure, the achieved accuracy in the air and total mass flux is good, and within 5% of the desired setting. The error in the fuel mass flux and the resulting equivalence ratio is much larger however, with an error of up to 8.1% in most cases and an error of 20.1% at the lowest fuel mass flux that was used. The error in the hydrogen mass flow explains the variation in the equivalence ratios that were achieved during testing.

The variation in the hydrogen mass flow is thought to be a result both of the fact that the total hydrogen mass flow is relatively low, but also the fact that the hydrogen mass flow is set using the supply pressure in a relatively long feed line. As discussed in Section 2.2 it can take some time for the pressure in the hydrogen supply line to be established, and with the short test times in the present test campaign this leads to a larger than desired variability in the achieved hydrogen mass flow. In future test campaigns the achieved equivalence ratio will therefore be verified after each test, and as testing continues to take place the fuel supply pressure will be adjusted to yield the desired equivalence ratio as best as possible.

Pressure gain

The pressure gain of the engine is calculated using the oxidiser stagnation pressure, obtained directly from a pressure measurement in the air plenum, and the stagnation pressure at the end of the detonation channel. The flow velocity in the air plenum is low and hence pressure that is measured in the plenum is assumed to be the total pressure. As discussed in Section 2.3 the total pressure at the end of the detonation channel is obtained from CTAP measurements, and example of which is shown in Figure 9 for a test with a total mass flow of 212 kg/s/m^2.

Copyright © 2024 by author(s)

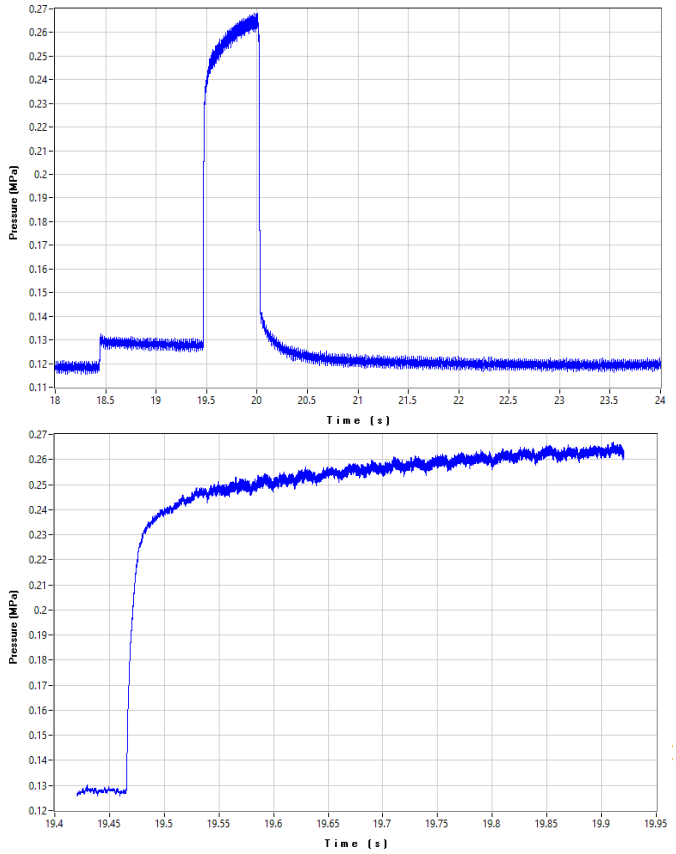

Figure 9 CTAP data for a test with a total mass flow of 212 kg/s/m^2. The figure at the top shows the 1s cold flow period, the 0.5s test and part of the test cool down, whereas the bottom figure only shows the 0.5s test.

At the top of the figure the CTAP data for the 1s cold flow period, the 0.5s test period and part of the cool down time is shown. The increase in pressure at t=18.42 corresponds to the start of fuel injection, while the increase of measured pressure at t≈19.48 s corresponds to engine ignition; this pressure increase occurs approximately 0.05 seconds after spark plug triggering at t=19.42s, which is in line with the average time required for the pre-detonator shock wave to enter the engine as discussed in Section 2.1. The significant increase in detonation channel pressure indicates successful ignition of the engine. The bottom of Figure 9 shows the data obtained during the test in more detail. The initial increase in pressure as the engine ignites is clearly visible, and the pressure appears to increase slightly during the test. It does start to plateau slightly towards the end of the test.

To calculate the pressure gain the average CTAP pressure during the last 350 ms of the test is used, to avoid capturing the initial start-up transients. As discussed in Section 2.3 the CTAP pressure is the static pressure, and it is converted to a total pressure using the Mach-area relation. Use of this relation assumes that the nozzle is choked, which is not true at all operating points; the nozzle is choked only when the total pressure at the CTAP location exceeds the critical pressure, which is approximately 1.89 bar for the atmospheric exhaust case considered here.

To filter out the cases for which the engine is not choked, the total pressure obtained by applying the Mach-area relation is compared to the ambient pressure. If this pressure is less than 1.89 times the ambient pressure the data point is omitted, and no pressure gain is calculated for this configuration. For the current test campaign the engine was not choked for 3 of the 12 successful hot fires, which had total mass flows between 51 kg/s/m^2 and 104 kg/s/m^2. This is in line with the results obtained for the TU Berlin RDC [8]. For all other tests a pressure gain could be calculated, and these values are shown in Figure 10

 Copyright © 2024 by author(s)

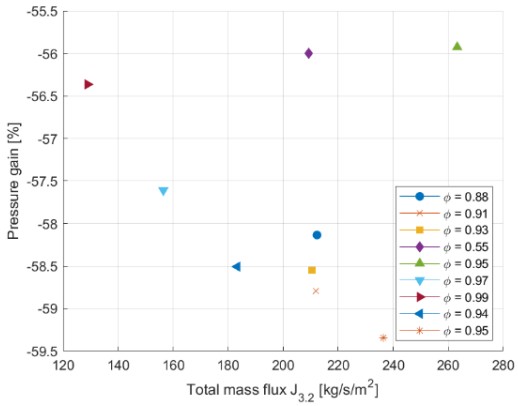

Figure 10 Achieved pressure gain as a function of total mass flux. The legend shows the equivalence ratio for each test.

The achieved pressure gain is between -55.5% and -59.5%, which is in line with the values obtained for the TU Berlin RDE [2]. The fact that the experimental data from this test campaign is in line with previously published experimental data for this engine geometry, in which pressure gain is measured using a Kiel probe, gives confidence in the operation of the facility and the diagnostics used on the TNO RDC.

Wave speed

Figure 11 shows the ionisation pin data for a typical test, which a total mass flow of 212 kg/s/m^2 and an equivalence ratio of 0.91. A Fast Fourier Transform (FFT) is applied to this data to obtain the signal frequency spectrum, which is also shown in the figure for each channel.

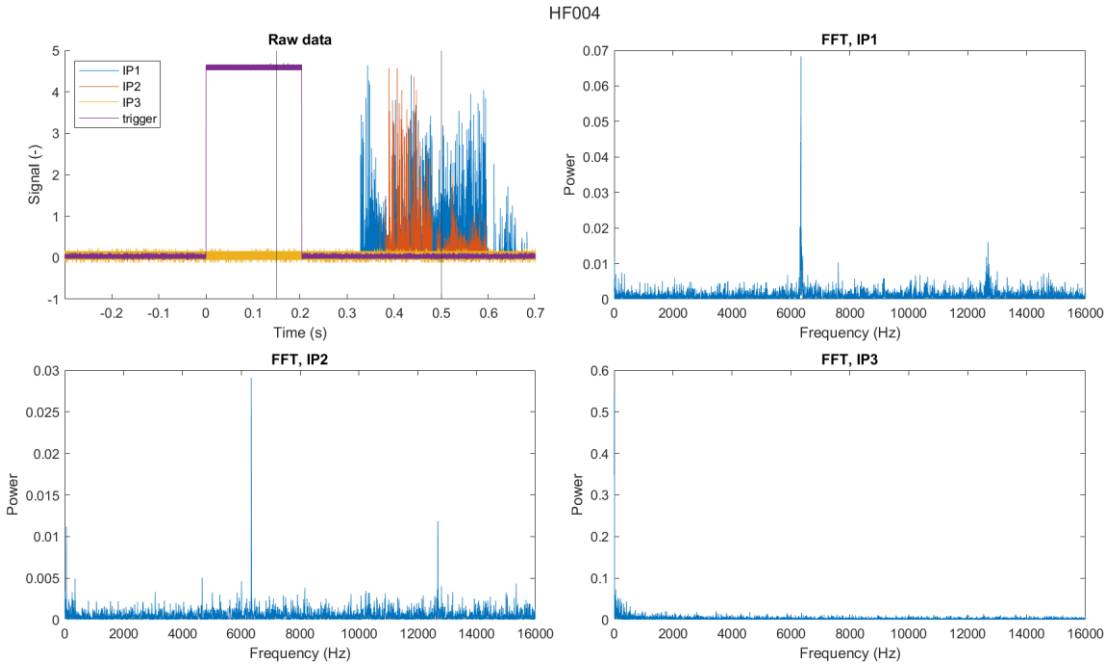

Figure 11 Ionisation probe data and FFTs for a test with a total mass flow of 212 kg/s/m^2 and an equivalence ratio of 0.91. The raw data is shown on the top left, while the FFTs of all channels are shown in the other figures. Note that for this test only IP1 and IP2 were connected to the engine. The vertical lines indicate the assumed end of the start-up transient (left line) and the end of the test (right line).

The top left of the figure shows the raw data for all oscilloscope channels. The first three channels are used to measure ionisation pin data, while the fourth channel is used to trigger the oscilloscope. The rising edge of this trigger, which is taken from the spark plug firing signal, marks the start of the test. As stated the test duration is 500 ms and engine startup is assumed to take 150 ms. The data between

Copyright © 2024 by author(s)

these two times, indicated by vertical lines in the top left figure, is used as input to the FFT. As is clear from Figure 11 the engine does not immediately shut down after the assumed end of the test because of the response time of the fuel shut off valve, but given that the supply valves are triggered after 500ms of test time the propellant conditions start to deviate from the operating point and this data is therefore not included in the analysis.

From the frequency spectra in Figure 11, there is a clear peak around 6400 Hz in both channels, with a smaller peak at 12800 Hz. Note that no pin was connected to the IP3 channel. The presence of strong peaks around 6400 Hz for both ionisation pins, as well as a weaker peak at a higher wave mode (the second in this case) of the combustion wave is an indication that there was a single detonation wave at this operating point, propagating at a frequency of 6400 Hz. This is in line with expectations from literature. Using the circumference of the engine, this translates to a wave speed of 1818 m/s, which is ~93% of the Chapman-Jouguet (CJ) velocity at that equivalence ratio.

Conversely, Figure 12 shows the spectrogram and frequency spectrum obtained from the sound of the same test.

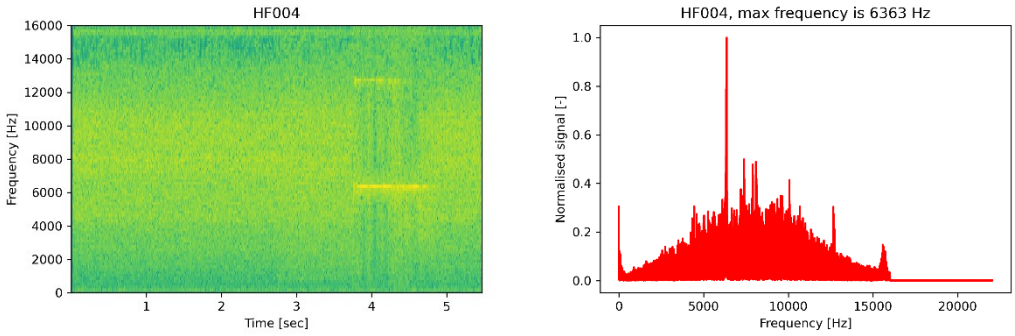

Figure 12 Video sound spectrogram (left) and FFT (right) for test HF-004.

The test appears to start at around 3.8 seconds, and the sound does not disappear until t≈4.6 seconds, i.e. a test duration of 800 milliseconds. As before, there is a clear peak in frequency around 6350 Hz, with a corresponding weaker peak at the second wave mode frequency. For this case the wave speed obtained from the ionisation pins and the sound analysis is therefore in agreement.

To highlight the differences between various engine operating modes, Figure 13 and Figure 14 show the sound analyses of two additional tests, with total engine mass flows of 78 kg/s/m^2 and 210 kg/s/m^2 and equivalence ratios of 1.03 and 0.42, respectively. In the first test there is a clear frequency peak at 4390 Hz, with associated smaller peaks around 7800 Hz and 8600 Hz. For the TNO RDC geometry these wave frequencies correspond to cases where the engine features two weak detonation waves with wave speeds close the speed of sound of the detonation products [8].

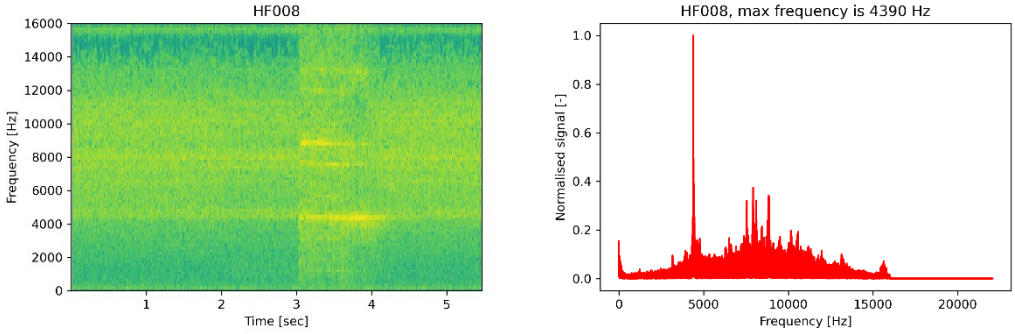

Figure 13 Video sound spectrogram (left) and FFT (right) for test HF-008.

In the second test the engine failed to ignite, as can be confirmed by examining the spectrogram on the left of Figure 14. The frequency spectrum in the figure does show some frequency peaks around

 Copyright © 2024 by author(s)

4000 and 8000 Hz, but the absolute signal strength is quite low. The peaks could be caused by the detonation waves deposited into the engine by the pre-detonator, which could have propagated for a short amount time before extinguishing. Given that the sound power is relatively low and the frequency spectrum is a lot noisier than for the other tests where the engine did successfully light, it is therefore likely that the engine did not ignite. Further evidence from e.g. a high speed camera is required to conclusively determine this however.

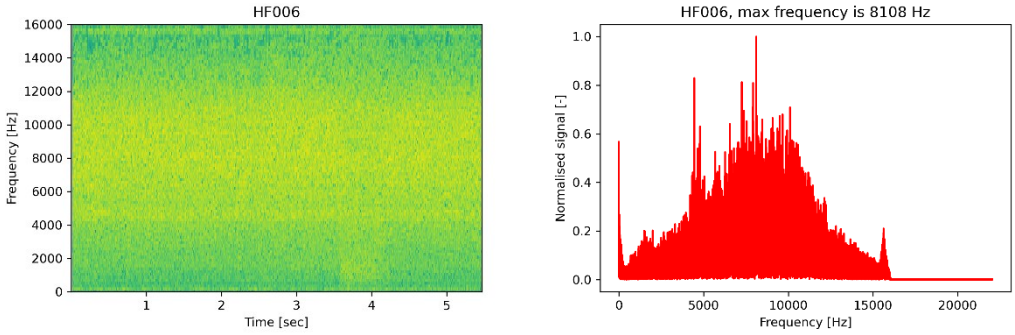

Figure 14 Video sound spectrogram (left) and FFT (right) for test HF-006.

Combining the frequency analyses of the ionisation pin data and the test video sound, the wave speed for each test is given in as a function of the CJ velocity. Note that the CJ velocity by which the wave speed is normalised is calculated for each test individually, using the equivalence ratio achieved in that test. Ionisation pin data is also not available for all tests, either because of sensors failing or the oscilloscope failing to be triggered.

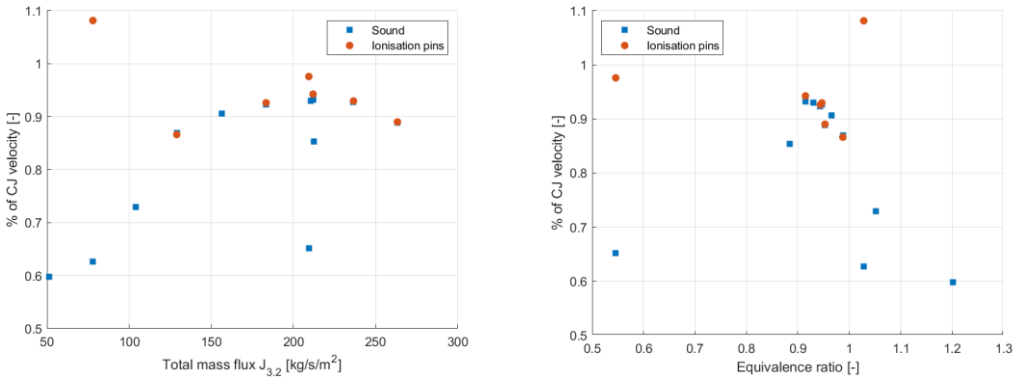

Figure 15 Wave speed as a function of CJ velocity as obtained from video sound (blue) and ionisation pins (orange) as a function of normalised total mass flux (left) and equivalence ratio (right).

Inspection of the figure shows that the wave speeds obtained from the ionisation pins and the sound analysis agree reasonably well in most cases. There are significant discrepancies for several cases however, particularly for the tests conducted at equivalence ratios of 0.55 and 1.04. For those tests the ionisation pin analysis predicts a wave speed in excess of the CJ velocity, and much higher than that predicted by the sound analysis.

In most of the tests the ionisation pins melted halfway during the tests, and because of the mounting plug that was used to install the plugs on the engine the pins sat in a small cavity where combustion products could circulate. Both factors can cause inaccuracies in the ionisation pin readings, and given that the wave speeds obtained from the ionisation pins appear to be erroneous (i.e. higher than the CJ velocity or in poor agreement with the sound analysis) in a number of cases an alternative to the ionisation pins will be used to measure wave speed in the future. The sound analysis results appear to be more reliable for the tests conducted as part of the test campaign described in this work, although the presence and size of the engine nozzle restriction could also influence the accuracy of the sound analysis.

Copyright © 2024 by author(s)

Examining the trends in Figure 15, the wave speed varies greatly depending on engine mass flow and operating mode, as expected. It appears to match the trend cited in the literature [8], transitioning from a two-wave mode with two weaker waves of equal strength (i.e. wave speeds of 60%-65% CJ velocity) to a two-wave mode with a stronger wave and a weaker wave (wave speed of 70-75% CJ velocity) to single strong wave mode (wave speeds of 90-95% CJ velocity). The effect of equivalence ratio on wave speed is also quite clearly shown in Figure 15, where there is a (significant) decrease is wave speed relative to the CJ velocity as equivalence ratio moves away from 0.95 to 1.

4. Conclusions

This work has reported on the RDE test facility that has been set up at TNO in the Netherlands. The facility consists of the modular TNO RDC, which is based on an RDC design from the literature, the propellant feed and control systems of TNO's existing aeropropulsion test facility and a custom-designed diagnostics suite. Each component of the test facility was described in detail, and the results of a commissioning campaign conducted with the TNO RDC were presented.

The pressure gain and detonation wave speed measurements obtained in the test campaign compared well to the results available in literature. This gives confidence in the ability of the engine diagnostics suite to quantify general RDC performance. The engine propellant mass flows were also found to be within 5% of the desired values, although the resulting equivalence ratio differed by up to 20% from the desired value in either direction. This is thought to be a result of the relatively high stoichiometric fuel-air ratio of hydrogen-air combustion, as well as the fact that the hydrogen feed line is relatively long and that its mass flow is controlled using pressure instead of mass flow. In the future the equivalence ratio achieved during each test will therefore be monitored more closely.

Some issues were also encountered with part of the engine diagnostics however, particularly with the ionisation pins and the high speed camera. The ionisation pin measurements were determined to be unreliable for a number of tests, likely because of the way they were mounted to the engine and the fact that they melted during tests in the majority of cases. The high speed camera was found to be insufficiently sensitive to detect the visible light emissions of the detonation wave. Alternatives for these diagnostic methods will therefore be explored for future test campaigns.

Testing of the TNO RDC is continuing in the future, at higher total engine mass flows and with more variations in test geometry. The engine diagnostics suite is also continuing to be developed, with the desire to incorporate in-situ pressure measurements in the detonation channel. These developments should also aid in gaining more experience with and confidence in the test facility, facilitating more diverse RDE studies in the future.

References

[1] R. Blümner, "Operating Mode Dynamics in Rotating Detonation Combustors," TU Berlin, 2019.

[2] E. Bach, C. Paschereit, P. Stathopoulos and M. Bohon, "Advancement of Empirical Model for Predicting Stagnation Pressure Gain in Rotating Detonation Combustors," in *AIAA SCITECH*, San Diego, CA, 2022.

[3] M. Bohon, R. Bluemner, C. Paschereit and E. Gutmark, "High-speed imaging of wave modes in an RDC," *Experimental Thermal and Fluid Science,* vol. 102, pp. 28-37, 2019.

[4] J. Shank, "Development and testing of a rotating detonation engine run on hydrogen and air," Air Force Institute of Technology, 2012.

[5] C. Brophy, J. Codoni, J. Teneyck and S. Ewing, "Experimental performance characterization of an RDE using Equivalent Available Pressure," in *AIAA Propulsion and Energy Forum*, Indianapolis, IN, 2019.

[6] D. Paxson and J. Hoke, "Time Averaged Pressure Measurements in Fundamentally Unsteady Pressure Gain Combustion Systems, NASA/TM-2013-217826," NASA, Cleveland, Ohio, 2013.

[7] S. Frolov, V. Aksenov, D. A.V., A. Zangiev, V. Ivanov, S. Medvedev and I. Shamsin, "Chemiionization and Acoustic Diagnostics of the Process in Continuous- and Pulse-Detonation Combustors," *Doklady Physical Chemistry,* vol. 1, no. Part 1, pp. 273-278, 2015.

 Copyright © 2024 by author(s)

[8] E. Bach, P. Stathopoulos, C. Paschereit and M. Bohon, "Performance Analysis of a Rotating Detonation Combustor based on Stagnation Pressure Measurements," *Combustion and Flame,* vol. 217, pp. 21-36, 2020.

 Copyright © 2024 by author(s)